

Origin of non-exponential relaxation in a crystalline ionic conductor: a multi-dimensional ^{109}Ag NMR study

M. Vogel, C. Brinkmann, H. Eckert, and A. Heuer

*Institut für Physikalische Chemie,
Westfälische Wilhelms-Universität,
Schlossplatz 4/7, 48149 Münster, Germany
and Sonderforschungsbereich 458*

(Dated: October 26, 2018)

The origin of the non-exponential relaxation of silver ions in the crystalline ion conductor $\text{Ag}_7\text{P}_3\text{S}_{11}$ is analyzed by comparing appropriate two-time and three-time ^{109}Ag NMR correlation functions. The non-exponentiality is due to a rate distribution, i.e., dynamic heterogeneities, rather than to an intrinsic non-exponentiality. Thus, the data give no evidence for the relevance of correlated back-and-forth jumps on the timescale of the silver relaxation.

PACS numbers: 64.70

Solid ion conductors are interesting materials from the viewpoints of both fundamental and applied science. While fast ion transport has important applications in energy and information technologies, many of its dynamic aspects are poorly understood at the atomic level. A prominent feature of many solid ion conductors is their non-exponential relaxation behavior, reflecting complex ion dynamics [1, 2, 3]. Two fundamentally different explanations are possible [4]. In the heterogeneous scenario, all particles are random-walkers, but a distribution of correlation times $G(\lg \tau)$ exists. In the homogeneous scenario, all particles obey the same relaxation function, which is, however, intrinsically non-exponential due to correlated back-and-forth jumps. For solid ion conductors, the concept of correlated forward-backward motion is one of the cornerstones of current modelling approaches. It is suggested by a strong frequency dependence of the electric conductivity $\sigma(\nu)$ [5, 6, 7]. Thus, it might be tempting to conclude that the homogeneous scenario applies to ion dynamics, i.e., ion transport might be slowed down by extended back-and-forth jump sequences.

Despite the technological importance of solid ion conductors, the origin of the non-exponential relaxation has remained unresolved to the present date. This is due to the fact that two-time correlation functions (2T-CF) such as scattering functions or conductivities are intrinsically unable to decide between both scenarios, but rather three-time correlation functions (3T-CF) are required [4]. The lifetimes of dynamic heterogeneities, if they exist, can be measured by four-time correlation functions (4T-CF). As was shown for applications in supercooled liquids [4, 8, 9], all of these multi-time correlation functions (MT-CF) are available from multi-dimensional NMR experiments. There, the 3T-CF has a simple interpretation: a dynamic filter meant to select slow particles is applied in the first time interval and the relaxation of the selected subset is observed in the second time interval. If dynamic heterogeneities exist, such a selection is possible and the

3T-CF decays more slowly than the regular 2T-CF.

For solid ion conductors, previous 2T-CF NMR studies have confirmed that relaxation is non-exponential [10, 11, 12, 13]. Moreover, it has been shown that MT-CF monitoring the diffusion of single silver ions can be recorded in ^{109}Ag NMR [12]. In this letter, we use multi-dimensional ^{109}Ag NMR to study for the first time the nature of the non-exponential relaxation in a solid ion conductor in detail. Specifically, we measure 3T-CF in polycrystalline $\text{Ag}_7\text{P}_3\text{S}_{11}$ to resolve the homogeneous and the heterogeneous contributions to the non-exponential silver ionic relaxation. Moreover, the lifetime of the dynamic heterogeneities is quantified by means of 4T-CF. $\gamma\text{-Ag}_7\text{P}_3\text{S}_{11}$ exhibits a high dc conductivity $\sigma_{dc} = 2.5 \times 10^{-4} \text{ S/cm}$ at $T \approx 300\text{K}$ [14]. We study silver dynamics in the β -phase below a phase transition at $T = 209\text{K}$ [15]. To improve the signal-to-noise ratio $\text{Ag}_7\text{P}_3\text{S}_{11}$ was synthesized starting from ^{109}Ag enriched (97%) metal powder. Further experimental details are described in Refs. [11, 12].

In solid-state ^{109}Ag NMR, the chemical shift (CS) interaction dominates the observed frequency shift, ω . The CS tensor describes the magnetic shielding of the applied static magnetic field \mathbf{B}_0 at the nuclear site due to neighboring electrons. In our case, fast silver rattling motions in the potential minimum affect the CS tensor so that a single, time-independent ω can be ascribed to each silver site. While the different local environments result in distinguishable values of ω , the NMR frequencies at sites related by translational symmetry are identical. Thus, any change in the resonance frequency is due to silver jumps between distinguishable sites. In other words, the sites within the unit cell provide a small number of NMR frequencies which are discontinuously adopted by the silver ions. ^{109}Ag NMR MT-CF directly probe the time dependence of ω and, hence, silver diffusion on the ms-s timescale. Since the values of ω associated with the silver sites depend on the orientation of the crystal with respect to \mathbf{B}_0 a powder average is observed for our poly-

crystalline sample.

The measurement of NMR MT-CF is well described in the literature [8, 9]. In general, suitable multi-pulse sequences are applied to manipulate the spin system. The pulses of these sequences divide the experimental time into a series of alternating short evolution times $t_p \ll \tau$ during which the respective NMR frequencies are detected and long mixing times $t_m \approx \tau$ during which dynamics may take place. The lengths and the phases of the pulses depend on the spin I of the observed nucleus. In our case $I = 1/2$, the multi-pulse sequences can be adopted from ^{13}C NMR experiments [8, 9, 16]. In detail, the three-pulse sequence $P_1 - t_p - P_2 - t_m - P_3 - t_p$, or stimulated-echo sequence, is used to record ^{109}Ag NMR 2T-CF. Varying t_m for constant t_p we measure

$$F_2^{cc}(t_m) \propto \langle \cos[\omega_1 t_p] \cos[\omega_2 t_p] \rangle \quad \text{and} \\ F_2^{ss}(t_m) \propto \langle \sin[\omega_1 t_p] \sin[\omega_2 t_p] \rangle.$$

Here, ω_1 and ω_2 are the frequencies during the two evolution times separated by the mixing time t_m . The brackets $\langle \dots \rangle$ denote ensemble averages. Suitable seven-pulse sequences can be applied to correlate the frequencies ω_1 , ω_2 , ω_3 and ω_4 during four evolution times t_p separated by three mixing times t_{m1} , t_{m2} and t_{m3} [8, 9, 16]. We record the 4T-CF

$$F_4(t_{m1}, t_{m2}, t_{m3}) \propto \langle \cos[(\omega_2 - \omega_1)t_p] \cos(\omega_3 t_p) \cos(\omega_4 t_p) \rangle,$$

which has proven very useful for a study of the lifetime of dynamic heterogeneities. A 3T-CF suited to analyze the origin of the non-exponential relaxation is obtained for $t_{m2} \rightarrow 0$ in the seven-pulse sequences, i.e., $\omega_3 = \omega_2$:

$$F_3(t_{m1}, t_{m3}) \propto \langle \cos[(\omega_2 - \omega_1)t_p] \cos(\omega_2 t_p) \cos(\omega_4 t_p) \rangle.$$

A straightforward interpretation of these MT-CF is possible when *each* silver jump to a distinguishable site leads to a complete loss of correlation. This condition can be met when large evolution times are applied so that $\Delta\omega t_p \gg 2\pi$ is fulfilled for basically all frequency changes resulting from these jumps. For $\Delta\omega t_p \gg 2\pi$, it is easily seen using the trigonometric addition theorems that

$$F_2(t_m) \equiv F_2^{cc}(t_m) = F_2^{ss}(t_m) \propto \langle \cos[(\omega_2 - \omega_1)t_p] \rangle \quad (1)$$

where the term $\cos[(\omega_2 - \omega_1)t_p]$ approximates the δ function $\delta(\omega_2 - \omega_1)$ [8, 9]. In ^{109}Ag NMR studies of $\text{Ag}_7\text{P}_3\text{S}_{11}$, Eq. 1 is fulfilled for $t_p \geq 100\mu\text{s}$ [11]. For such evolution times, independent of the actual value of t_p , $F_2(t_m)$ quantifies the fraction of ions that occupy the same or – due to the identical ω – any periodic site after a time t_m . Similarly, one can rewrite

$$F_3(t_{m1}, t_{m3}) \propto \langle \cos[(\omega_2 - \omega_1)t_p] \cos[(\omega_4 - \omega_2)t_p] \rangle \quad \text{and} \quad (2)$$

$$F_4(t_{m1}, t_{m2}, t_{m3}) \propto \langle \cos[(\omega_2 - \omega_1)t_p] \cos[(\omega_4 - \omega_3)t_p] \rangle. \quad (3)$$

In studies of glassy ion conductors, i.e., in the absence of periodic sites, the term $\cos[(\omega_2 - \omega_1)t_p]$ acts as a perfect

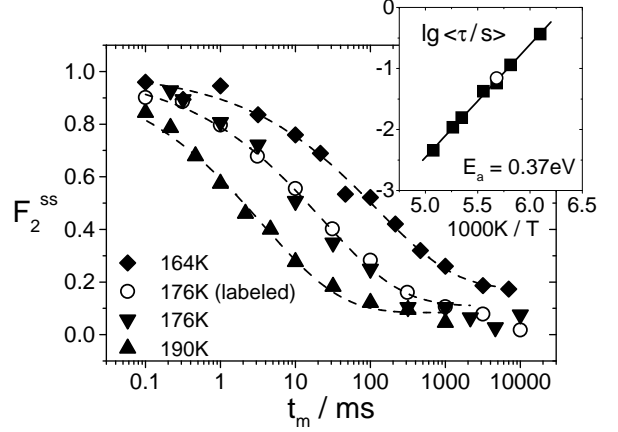


FIG. 1: $F_2^{ss}(t_m)$ for polycrystalline $\text{Ag}_7\text{P}_3\text{S}_{11}$ at various temperatures ($t_p = 100\mu\text{s}$). We compare results for samples containing 48% ^{109}Ag (solid symbols, Ref. [11]) and 97% ^{109}Ag (open symbols), respectively. The dashed lines are interpolations with a modified KWW function. Inset: Mean correlation times $\langle \tau \rangle$ together with an Arrhenius interpolation.

dynamic filter which selects immobile ions during t_{m1} ($\omega_2 = \omega_1$). Then, the relaxation of these selected ions is observed via $F_3(t_{m3})$ so that $F_3(t_{m3}) \neq F_2(t_{m3})$ directly indicates the existence of dynamic heterogeneities. Further, the lifetime of dynamic heterogeneities can be measured when $F_4(t_{m2})$ for $t_{m1} = t_{m3} = \text{const.}$ is recorded. In this experiment, identical filters are applied to probe the dynamic states of an ion during t_{m1} and a time t_{m2} later during t_{m3} so that an exchange of the dynamic state results in a decay of $F_4(t_{m2})$, cf. below. Here, we will demonstrate that although the lattice periodicity leads to imperfect dynamic filters in applications on crystalline ion conductors $F_3(t_{m3})$ and $F_4(t_{m2})$ still yield valuable insights into the nature of silver dynamics in $\text{Ag}_7\text{P}_3\text{S}_{11}$.

In Fig. 1, we show ^{109}Ag NMR 2T-CF for $\text{Ag}_7\text{P}_3\text{S}_{11}$ at selected temperatures. The silver jumps lead to temperature dependent, non-exponential decays of $F_2(t_m)$. Experiments for the labelled sample and for a sample with natural isotopic abundance [11] yield identical results. Fitting to a modified Kohlrausch-Williams-Watts (KWW) function [17], $(1 - C) \exp[-(t/\tau)^\beta] + C$, the non-exponentiality is reflected by a stretching parameter of $\beta = 0.42$. The plateau value $C \approx 0.12 \approx 1/8$ indicates eight occupied, magnetically distinguishable silver sites [11]. The mean correlation time can be calculated according to $\langle \tau \rangle = (\tau/\beta) \Gamma(1/\beta)$ where $\Gamma(x)$ is the Γ function. Its temperature dependence is well described by an Arrhenius law with activation energy $E_a = 0.37\text{eV}$, see inset. We carefully checked that neither spin-lattice relaxation ($T_1 \approx 30\text{s}$) nor spin diffusion affect the data for mixing times shorter than about a few seconds.

The origin of the non-exponential silver dynamics in $\text{Ag}_7\text{P}_3\text{S}_{11}$ is revealed by $F_3(t_{m3})$. It is shown in Fig. 2 for the dynamic filters $t_{m1} = 10\text{ms}$, 40ms and $T = 176\text{K}$. In

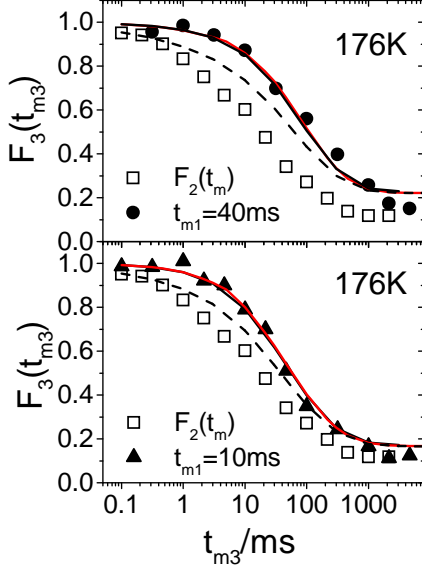


FIG. 2: $F_3(t_{m3}; t_{m1})$ for $\text{Ag}_7\text{P}_3\text{S}_{11}$ at $T = 176\text{K}$ ($t_p = 200\mu\text{s}$). The results for $t_{m1} = 10\text{ms}$, 40ms are compared with $F_3(t_{m3}; t_{m1} \rightarrow 0) \approx F_2^{\text{sc}}(t_{m3}) \approx F_2(t_{m3})$. The respective expectations for purely homogeneous dynamics (dashed lines) and purely heterogeneous dynamics (solid lines) are included. The expectations for heterogeneous dynamics in the O-model (black) and the D-model (gray) are nearly identical.

particular for the longer t_{m1} , $F_3(t_{m3})$ decays much more slowly than $F_2(t_{m3})$. In studies of supercooled liquids, the theoretical expectations for purely heterogeneous dynamics, $F_3^{\text{het}}(t_{m3})$, and purely homogeneous dynamics, $F_3^{\text{hom}}(t_{m3})$, can be expressed in a model-free way based on the measured 2T-CF [18, 19, 20]. For $\text{Ag}_7\text{P}_3\text{S}_{11}$, the presence of a small number of discrete NMR frequencies, which are discontinuously adopted, complicates the analysis. In general, one has to specify the crossover paths between the different sites/ ω to define the purely heterogeneous and the purely homogeneous scenario. Since detailed information is not available, we restrict ourselves to the analysis of two extreme cases. For reasons of simplicity, we assume that there are eight distinguishable sites on a cubic lattice. While the frequencies of every other site in each dimension are identical in the ordered (O-) model, the $N \approx 8$ values of ω are randomly distributed in the disordered (D-) model.

For the following calculations, it is useful to rewrite $F_3 \propto 1/2\{\langle \cos[(\omega_1 - \omega_4)t_p] \rangle + \langle \cos[(\omega_1 + \omega_4 - 2\omega_2)t_p] \rangle\}$. Since $\Delta\omega t_p \gg 2\pi$, ions showing $\omega_1 = \omega_4$ and $\omega_1 = \omega_2 = \omega_4$ contribute to the first and the second term, respectively. We denote $p^k(t)$ as the probability that after a time t an ion occupies a site with identical NMR frequency. If dynamic heterogeneities exist, this probability depends on the jump rate as indicated by the index k . In general, we can write

$$F_2(t_m) = \langle p^k(t_m) \rangle \text{ and} \quad (4)$$

$$F_3(t_{m1}, t_{m3}) = 1/2 \langle p^k(t_{m1} + t_{m3}) + p^k(t_{m1})p^k(t_{m3}) \rangle. \quad (5)$$

Here, the brackets denote the average over the rate distribution $G(k)$ that is present in the case of dynamic heterogeneities, but becomes a delta-function for purely homogeneous dynamics.

The homogeneous limit can be discussed in a model-free way. Since a rate distribution is absent, one directly has $p^k(t) = F_2(t)$ and, thus,

$$F_3^{\text{hom}}(t_{m1}, t_{m3}) = (1/2)[F_2(t_{m1} + t_{m3}) + F_2(t_{m1})F_2(t_{m3})]. \quad (6)$$

For the heterogeneous limit, we first discuss the O-model. In this case, one can specify $p^k(t)$ from simple arguments. For a jump rate k and one-dimensional dynamics, the probability to be at a site with the same NMR frequency is $(1/2)[1 + \exp(-2kt)]$ [18]. Since the dynamics along the different dimensions are independent of each other $p^k(t) = \{(1/2)[1 + \exp(-2kt)]\}^3$ follows. Using this expression for $p^k(t)$ one can determine the distribution $G(k)$ from Eq. 4 and use it to calculate $F_3^{\text{het}, O}$ via Eq. 5. Now, we turn to the heterogeneous scenario of the D-model. For a single jump rate k , one has

$$p^k(t_m) = \frac{1}{N} + \left(1 - \frac{1}{N}\right) \exp(-kt_m). \quad (7)$$

With this choice of $p^k(t_m)$, Eq. 5 can be rewritten as

$$F_3^{\text{het}, D}(t_{m1}, t_{m3}) = F_2(t_{m1} + t_{m3}) + \frac{1}{2N}[F_2(t_{m1}) + F_2(t_{m3}) - F_2(t_{m1} + t_{m3}) - 1]. \quad (8)$$

Actually, we use $N = 8.4$ for the D-model where this value results from a fit of Eq. 4 to the experimental data.

In Fig. 2, we see that the experimental data for $t_{m1} = 10\text{ms}$, 40ms agree well with $F_3^{\text{het}}(t_{m3})$ obtained within both the O-model and the D-model. The minor deviations in the plateau regime ($t_{m3} > 1\text{s}$) are likely due to an onset of spin diffusion. In contrast, $F_3^{\text{hom}}(t_{m3})$ distinctly deviates from the experimental results. The agreement of both limiting cases with respect to the heterogeneous limit clearly shows that, as is the case for supercooled liquids, the heterogeneous limit can be characterized in a basically model-free manner. We conclude that correlated back-and-forth jumps on the timescale of the silver relaxation are not a relevant feature of the dynamics.

Finally, the lifetime of the dynamic heterogeneities in $\text{Ag}_7\text{P}_3\text{S}_{11}$ is measured by recording $F_4(t_{m2})$ for $t_{m1} = t_{m3} = t_s \approx \tau$. If there were perfect dynamic filters, slow silver ions ($\tau > t_s$) would be selected during t_{m1} and a time t_{m2} later it would be checked whether these ions are in the same dynamical state during t_{m3} , cf. Eq. 3. Thus, $F_4(t_{m2})$ would decrease when initially slow ions become fast ($\tau < t_s$) during t_{m2} until the re-equilibration of the respective subensemble is complete. In our case, the signal results from all ions showing $\omega_1 = \omega_2$ and $\omega_3 = \omega_4$

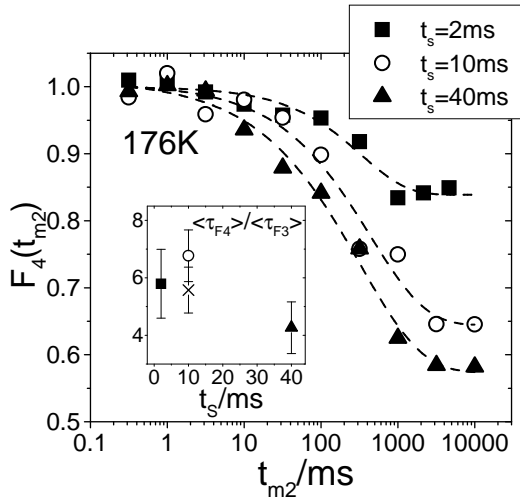


FIG. 3: $F_4(t_s, t_{m2}, t_s)$ for $\text{Ag}_7\text{P}_3\text{S}_{11}$ at $T=176\text{K}$ ($t_p=200\mu\text{s}$). The filter times t_s are indicated. Lines: Interpolations with a modified KWW function. The inset shows the scaled mean decay times $\langle\tau_{F4}\rangle/\langle\tau_{F3}\rangle$. For comparison, one data point for $T=182\text{K}$ is included (X). For $t_s = 2\text{ms}$ and for $T=182\text{K}$ $\langle\tau_{F3}\rangle$ has been estimated from F_3^{het} , as calculated using Eq. 8.

so that fast ions that occupy periodic sites at the relevant times contribute, too. Detailed random-walk simulations based on the O- and the D-model have shown, however, that despite the imperfection of the dynamic filter $F_4(t_{m2})$ is well suited to measure the timescale of exchange processes between fast and slow ions.

The curves $F_4(t_{m2})$ for $\text{Ag}_7\text{P}_3\text{S}_{11}$ at $T=176\text{K}$ and various t_s are shown in Fig. 3. Non-exponential decays to different plateau values for $t_{m2} \rightarrow \infty$ indicate exchange processes between slow and fast silver ions until the re-equilibration of the respective subensemble is complete. To quantify the exchange rate the decays are fitted to a modified KWW function. We obtain mean time constants $\langle\tau_{F4}\rangle = 390\text{--}660\text{ms}$ that do not significantly depend on the filter time t_s . These values are on the same order as $\langle\tau_{F3}\rangle$ and, hence, the exchange processes between slow and fast ions of the distribution occur on the timescale of the slow silver jumps. However, as indicated by $\langle\tau_{F4}\rangle/\langle\tau_{F3}\rangle \approx 6$, see inset, it takes a few rather than a single jump relaxation process to loose memory about the mobility, suggesting that high and low energy barriers are not randomly distributed in the unit cell of $\text{Ag}_7\text{P}_3\text{S}_{11}$.

In summary, the observation of NMR MT-CF provides valuable insights into the mechanism of ion motion, not available by other experimental methods. The silver jumps in the crystalline ion conductor $\text{Ag}_7\text{P}_3\text{S}_{11}$ are governed by a broad rate distribution within which exchange processes between slow and fast ions take place on the timescale of the slow jumps. Further, the purely heterogeneous scenario applies to the relaxation of the

non-fast silver ions and, hence, back-and-forth jumps are not relevant on the time scale of the depopulation of the silver sites. At first sight, this seems to contradict the presence of back-and-forth motions inferred from the frequency dependent electric conductivity $\sigma(\nu)$. Both results might be reconciled if one assumes that only very fast ions contribute to the dispersion of $\sigma(\nu)$, whereas ionic motion on the typical timescale of the silver relaxation is random-walk like. This conclusion is backed up by MD simulations on glassy ion conductors where the back-jump probability was found to depend strongly on the waiting times at the sites [21, 22].

Funding of the Deutsche Forschungsgemeinschaft (DFG) through the Sonderforschungsbereich 458 is gratefully acknowledged. M. V. thanks the DFG for funding through the Emmy Noether-Programm.

-
- [1] C. T. Moynihan, L. P. Boesch and N. L. Laberge, Phys. Chem. Glasses 14, 122 (1973)
 - [2] C. Liu and C. A. Angell, J. Non-Cryst. Solids 83, 162 (1986)
 - [3] D. L. Sidebottom, P. F. Green and R. K. Brow, J. Non-Cryst. Solids 183, 151 (1995)
 - [4] R. Böhmer, R. V. Chamberlin, G. Diezemann, B. Geil, A. Heuer, G. Hinze, S. C. Kuebler, R. Richert, B. Schiener, H. Sillescu, H. W. Spiess, U. Tracht and M. Wilhelm, J. Non-Cryst. Solids 235-237, 1 (1998)
 - [5] A. K. Jonscher, Nature 267, 673 (1977)
 - [6] M. D. Ingram, Phys. Chem. Glasses 28, 215 (1987)
 - [7] B. Roling, A. Happe, K. Funke and M. D. Ingram, Phys. Rev. Lett. 78, 2160 (1997)
 - [8] K. Schmidt-Rohr and H. W. Spiess, Multidimensional Solid-State NMR and Polymers, Academic Press, London (1994)
 - [9] R. Böhmer, G. Hinze, G. Diezemann and E. Rössler, Prog. Nucl. Magn. Reson. Spectrosc. 39, 191 (2001)
 - [10] R. Böhmer, T. Jörg, F. Qi and A. Titze, Chem. Phys. Lett. 316, 419 (2000)
 - [11] M. Vogel, C. Brinkmann, H. Eckert and A. Heuer, J. Non-Cryst. Solids 307-310, 971 (2002)
 - [12] M. Vogel, C. Brinkmann, H. Eckert and A. Heuer, Phys. Chem. Chem. Phys. 4, 3237 (2002)
 - [13] F. Qi, T. Jörg and R. Böhmer, Solid State Nucl. Magn. Reson. 22, 484 (2002)
 - [14] Z. Zhang and J. H. Kennedy, J. Electrochem. Soc. 140, 2384 (1993)
 - [15] C. Brinkmann, M. Vogel, H. Eckert, A. Heuer and A. Pfitzner, unpublished results
 - [16] U. Tracht, M. Wilhelm, A. Heuer and H. W. Spiess, J. Magn. Reson. 140, 460 (1999)
 - [17] R. Kohlrausch, Pogg. Ann. Phys. 4, 56 (1854); G. Williams and D.C. Watts, Trans. Faraday Soc. 66, 80 (1970)
 - [18] A. Heuer, U. Tracht, S. C. Kuebler and H. W. Spiess, J. Molec. Structure 479, 251 (1999)
 - [19] U. Tracht, PhD Thesis, University of Mainz, Germany, 1998
 - [20] A. Heuer and K. Okun, J. Chem. Phys. 106, 6176 (1997)

- [21] H. Lammert, M. Kunow and A. Heuer, Phys. Rev. Lett. 90, 215901 (2003)
- [22] M. Vogel, Phys. Rev. B (in press)